



Molecular Biology

Two poplar cellulose synthase-like D genes, *PdCSLD5* and *PdCSLD6*, are functionally conserved with *Arabidopsis CSLD3*

Guang Qi^{a,b,1}, Ruibo Hu^{a,1}, Li Yu^a, Guohua Chai^a, Yingping Cao^a, Ran Zuo^a, Yingzhen Kong^c, Gongke Zhou^{a,*}

^a Key Laboratory of Biofuels, Shandong Provincial Key Laboratory of Energy Genetics, Qingdao Institute of Bioenergy and Bioprocess Technology, Chinese Academy of Sciences, Qingdao 266101, PR China

^b University of Chinese Academy of Sciences, Beijing 100049, China

^c Complex Carbohydrate Research Center, The University of Georgia, 315 Riverbend Road, Athens, GA 30602, USA

ARTICLE INFO

Article history:

Received 30 November 2012

Received in revised form 1 April 2013

Accepted 7 April 2013

Available online 5 June 2013

Keywords:

Cellulose synthase-like D

Crystalline cellulose

Poplar

Root hair

ABSTRACT

Root hairs are tip-growing long tubular outgrowths of specialized epidermal cells, and are important for nutrient and water uptake and interaction with the soil microflora. Here we characterized two poplar *cellulose synthase-like D* (*CSLD*) genes, *PdCSLD5* and *PdCSLD6*, the most probable orthologs to the *Arabidopsis AtCSLD3/KOJAK* gene. Both *PdCSLD5* and *PdCSLD6* are strongly expressed in roots, including in the root hairs. Subcellular localization experiments showed that these two proteins are located not only in the polarized plasma membrane of root hair tips, but also in Golgi apparatus of the root hair and non-hair-forming cells. Overexpression of these two poplar genes in the *atcsld3* mutant was able to rescue most of the defects caused by disruption of *AtCSLD3*, including root hair morphological changes, altered cell wall monosaccharide composition, increased non-crystalline β-1,4-glucan and decreased crystalline cellulose contents. Taken together, our results provide evidence indicating that *PdCSLD5* and *PdCSLD6* are functionally conserved with *AtCSLD3* and support a role for *PdCSLD5* and *PdCSLD6* specifically in crystalline cellulose production in poplar root hair tips. The results presented here also suggest that at least part of the mechanism of root hair formation is conserved between herbaceous and woody plants.

© 2013 Elsevier GmbH. All rights reserved.

Introduction

Root hairs are polarized, tip-growing and tubular outgrowths of specialized root epidermal cells called trichoblasts (Dolan et al., 1994), which are important for the uptake of water and nutrients, and also serve as the interface between the plant and soil microbe (Peterson, 1992). Root hair development was divided into three structural phases: cell specification, initiation and elongation. In this process, rapid cell wall assembly at the growing tip is required for the root hair development since growing hairs can be deformed or ruptured at the very tips when any cell wall components are missing or disrupted (Fahey et al., 2001; Foreman and Dolan, 2001; Carol and Dolan, 2002; Galway, 2006). The cell wall at root hair tips mainly comprises primary cell wall, with similar polysaccharide composition to other cells, consisting typically of cellulose,

hemicelluloses and pectins (Somerville et al., 2004; Galway, 2006; Lerouxel et al., 2006).

Understanding the synthesis of cell walls has attracted considerable interests, not only because of their biological functions, but also due to their extensive applied uses as food ingredients, fiber and biofuel feedstocks. Cellulose is one of the main components of cell walls and is thought to be synthesized by cellulose synthase (CESA) family (Somerville et al., 2004; Lerouxel et al., 2006). In *Arabidopsis*, there are ten CESAs (Richmond and Somerville, 2000), and their roles in cell wall synthesis have been extensively characterized (Taylor et al., 2003; Desprez et al., 2007; Persson et al., 2007). These proteins reside in plasma membrane-embedded complexes termed rosettes for cellulose synthesis (Somerville et al., 2004). Previous research showed that *Arabidopsis* root hairs rupture at their tips when treated with 2,6-dichlorobenzonitrile (DCB), an inhibitor of cellulose synthesis, indicating that cellulose is required for the integrity of cell walls at the hair tips, and mutations of the CESAs at the root hair tips are expected to result in the rupture of root hairs (Fahey et al., 2001; Carol and Dolan, 2002). However, so far, there is no report concerning the essential roles of CESA proteins for cellulose synthesis in tip-growing root hairs (Caño-Delgado et al., 2003; Singh et al., 2008), suggesting that cellulose at root hair tips is synthesized by

Abbreviations: CSL, CESA-like; GUS, β-glucuronidase; qRT-PCR, quantitative real-time RT-PCR; GFP, green fluorescent protein.

* Corresponding author. Tel.: +86 532 80662731; fax: +86 532 80662778.

E-mail address: zhougk@qibebt.ac.cn (G. Zhou).

¹ These authors contributed equally to this work.

glycosyltransferases (GT) that are not classified within the CESA family.

Cellulose synthase-like (CSL) proteins were identified by the sequence similarity to CESAs. There are 29 CSL genes in *Arabidopsis*, while at least 30 putative CSL genes in poplar (Suzuki et al., 2006). The *Arabidopsis* CSL gene family can be divided into six subfamilies namely *CSLA*, *CSLB*, *CSLC*, *CSLD*, *CSLE* and *CSLG* (Richmond and Somerville, 2000). Two additional subfamilies (*CSLF* and *CSLH*) have been found exclusively in grasses (Lerouxel et al., 2006) and another subfamily (*CSLJ*) is present in grasses and some dicot species (Fincher, 2009). Various CSL proteins have been shown to be involved in synthesizing backbone of hemicelluloses (Dhugga et al., 2004; Liepman et al., 2005; Burton et al., 2006, 2008; Lerouxel et al., 2006; Cocuron et al., 2007; Bernal et al., 2008; Park et al., 2011). Among the CSL genes, *CSLD* family has the highest sequence similarity to CESAs, which indicates that CSLDs may also function as cellulose synthases to synthesize β -1,4-linked glucan chains (Doblin et al., 2001; Richmond and Somerville, 2001).

Clues to the biological functions of the CSLs have been sought widely by defining their biochemical activity and/or subcellular localization, but interpretation of this work has not yet been conclusive. There is a growing body of evidence showed that the CSLDs participated in specific polysaccharide synthesis in tip growth and stem development, and several mutants of *Arabidopsis* *CSLD* family have severe phenotypic defects. Two *Arabidopsis* *CSLD* genes, *AtCSLD2* and *AtCSLD3/KOJAK*, are specifically involved in root hair formation (Favery et al., 2001; Wang et al., 2001; Bernal et al., 2008; Galway et al., 2011; Park et al., 2011). Root hairs of *atcsld3* mutant rupture during outgrowth, while *atcsld2* mutant hairs rupture later, during tip growth, and the defective root hair phenotype of *atcsld3* could be recovered by overexpression of *AtCSLD2* (Yin et al., 2011), suggesting partial functional redundancy of the two genes. Recent progress has proposed a role for *AtCSLD3* with a distinct (1→4)- β -glucan synthase activity in apical plasma membranes during root hair tip growth (Park et al., 2011). In addition, *AtCSLD2* and *AtCSLD3* are also indicated to play a role in female gametophyte development (Yoo et al., 2012). The *atcsld5* mutant has moderately reduced growth due to lower activity of synthesis of xylan and pectin rather than a specific polymer (Bernal et al., 2007), while both *atcsld1* and *atcsld4* mutants are deficient in pollen tube growth (Bernal et al., 2008). Mutation in *OcCSLD1* exhibits similar changes in root hair formation as *atcsld3* (Kim et al., 2007). *NaCSLD1* was shown to be required for the formation of cell wall in developing pollen tubes of tobacco (Doblin et al., 2001). In particular, *ZmCSLD1* reveals a previously unrecognized role for CSLDs in plant cell division, especially during early phases of cross-wall formation (Hunter et al., 2012).

In this study, to functionally characterize the root hair-specific *CSLD* genes, two poplar *CSLD* genes, *PdCSLD5* and *PdCSLD6*, were subjected to molecular and genetic identification. We examined their expression and subcellular localization patterns, tested their abilities to complement the defects of *atcsld3* mutant, and gain further insight into functions of CSLDs by cell wall sugar composition analysis. Our results provide evidences showing that *PdCSLD5* and *PdCSLD6* are functionally conserved with *AtCSLD3* and support a role for *PdCSLD5* and *PdCSLD6* specifically in crystalline cellulose synthesis in poplar root hair tips.

Materials and methods

Plant materials and growth conditions

One-year-old poplar (*Populus deltoides*) was grown in greenhouse under 16 h light/8 h dark at 25–28 °C. Shoot apices (internodes 1–3 from top, same as below), leaf (from internodes 4–6), developing xylem (from the basal internodes), phloem (from the basal

internodes), cortex (from the basal internodes), young and old roots were harvested separately. All samples were immediately frozen in liquid nitrogen and stored at –80 °C until further process.

Arabidopsis thaliana ecotype Columbia (Col-0) was used in this study. The T-DNA insertion line SALK_112105 (*atcsld3*) was obtained from Nottingham *Arabidopsis* Stock Centre (NASC, Nottingham, UK). *Arabidopsis* plants were grown in greenhouse under 16 h light/8 h dark at 22 °C with 65% relative humidity. Seeds were sterilized before sown on half strength MS medium. After stratification at 4 °C for 2 d, *Arabidopsis* seeds were germinated at 22 °C.

Bioinformatic analyses of *CSLD* protein sequences

Multiple alignment analysis of the full-length protein sequences was performed by Clustal X (version 1.83) program (Thompson et al., 1997). The unrooted phylogenetic tree was constructed with MEGA 4.0 program using the Neighbor-Joining (NJ) method with 1000 bootstrap replicates (Tamura et al., 2007). Synteny information was collected from the Plant Genome Duplication Database (PGDD; <http://chibba.agtec.uga.edu/duplication>).

Quantitative real-time PCR

Total RNA extraction and quantitative real-time PCR (qRT-PCR) was conducted as described previously (Hu et al., 2010). The expression of the ubiquitin gene (*UBQ10*, BU879229) was used as an internal control. The primers used to amplify the transcripts were as follows: 5'-CGAACACTCCAGAAGAGAAC-3' and 5'-CTCTGTCACTGGGATTGAGT-3' for *PdCSLD5*; 5'-CCTATCAACTAG-CTCGGATG-3' and 5'-GATCATCCCTTGAGTAGCTG-3' for *PdCSLD6*; 5'-GTTGATTTGCTGGGAAGC-3' and 5'-GATCTGGCCTCACGTT-GT-3' for *UBQ10*.

In situ hybridization

In situ hybridization was performed as previously described (Zhou et al., 2007). Briefly, poplar roots were fixed in 2.5% formaldehyde and 0.5% glutaraldehyde and embedded in paraffin. Sections (10 μ m thick) were cut, mounted on glass slides and hybridized with digoxigenin-labeled *PdCSLD5* and *PdCSLD6* antisense or sense RNA probes. The hybridization signals were detected by incubating with alkaline phosphatase-conjugated antibodies against digoxigenin and subsequent color development with alkaline phosphatase substrates. For the synthesis of antisense and sense probes used for *in situ* hybridization, a 210 bp fragment of *PdCSLD5* cDNA and a 198 bp fragment of *PdCSLD6* cDNA were PCR amplified with their corresponding primers (5'-GGATTGTGATCATTGTCATGAT-3' and 5'-GAATCAATTCAAATATCCG-3' for *PdCSLD5*; 5'-CCATTTCAGGCAGATGACT-3' and 5'-ATTGAGACAACCTCGGACACG-3' for *PdCSLD6*). The RNA probes were synthesized with the DIG RNA labeling mix (Roche, Mannheim, Germany) according to the manufacturer's instruction, respectively.

GUS expression assays

To generate *pPdCSLD5::GUS* and *pPdCSLD6::GUS* transgenic plants, 2015 bp and 2003 bp genomic fragment upstream of the putative ATG start codon of *PdCSLD5* and *PdCSLD6* were PCR amplified using their corresponding primers (5'-CCCCAACAAACTCCGATTA-3' and 5'-GAGCTCCGATTGTCTCTG-3' for *PdCSLD5*; 5'-GATTGTCACTATATTGATAAAC-3' and 5'-ATTTAACACTATAAGAGACTTC-3' for *PdCSLD6*), and subcloned into the upstream of *GUS* gene in pKGWFS7 vector (Karimi et al., 2002), respectively. The resulting constructs were transformed into wild type (WT) *Arabidopsis* plants, and the T1 transgenic plants were

used for GUS activity analysis. GUS staining was performed as described previously (Jefferson et al., 1987).

Mutant complementation analysis

The full-length *PdCSLD5* and *PdCSLD6* cDNAs were isolated by RT-PCR from *Populus deltoides* young root-derived cDNAs, with their corresponding primers (5'-ATGGCCTCAAGATCATCAAAG-3' and 5'-TCAGGGAAACTGGAATGAGCCA-3' for *PdCSLD5*; 5'-ATGGCC-TCAAATCATTCAAGG-3' and 5'-TCAAGGAAACTGGAAGAGGCC-3' for *PdCSLD6*). The amplified fragments were ligated to the Gateway entry vector pGWC-T as described previously (Chen et al., 2006), sequenced and then transferred into the Gateway binary vector pH2GW7 (Karimi et al., 2002) using the Gateway recombination system (Invitrogen) according to the manufacturer's instructions.

For complementation analysis, the constructs were introduced into the *Arabidopsis atcsld3* mutant plants. Transgenic plants were selected on hygromycin, and verified by PCR. The first generation of transgenic plants was used for morphological and anatomical analyses.

Subcellular localization of GFP-tagged *PdCSLD5* and *PdCSLD6*

The *PdCSLD5* and *PdCSLD6* coding regions were cloned in frame with an enhanced green fluorescent protein (EGFP) gene under the control of the CaMV 35S promoter in pK7WGF2 to generate the N-terminal fusion constructs 35S-GFP-*PdCSLD5* and 35S-GFP-*PdCSLD6*. The resulting recombinant vectors were sequenced and then transformed individually into WT *Arabidopsis* plants.

FM4-64 staining was conducted as described previously (Jelinkova et al., 2010). Roots of 4-day-old transgenic seedlings were primed for 2–6 min with 2 μM FM4-64 in dark, then rinsed three times in liquid MS medium, and analyzed by confocal microscopy. Co-infiltrations of *Nicotiana benthamiana* leaves with mCherry-tagged Man49 (Nelson et al., 2007) and GFP-tagged *PdCSLD5* or *PdCSLD6* were performed as described previously (Bernal et al., 2007). Signals of FM4-64, GFP and mCherry were observed using a Laser Scanning Confocal Microscope (OLYMPUS FV1000).

Immunohistochemistry

4-day-old seedlings, with roots 10–12 mm in length, were fixed, dehydrated, and embedded in LR White resin (Ted Pella Inc., Redding, CA) as described previously (Cavalier et al., 2008). Sections (250 nm) were cut with an Ultracut E ultramicrotome (Leica). For immunochemical staining using the monoclonal antibodies, sections were incubated with the monoclonal antibody, and then with 1:100 diluted goat anti-mouse-FITC- or anti-rat-FITC-conjugated secondary antibody (Invitrogen). For detection using CBMs, after incubated with CBMs, sections were incubated with 100-fold dilution of mouse anti-HIS monoclonal antibody, and then with 1:100 diluted goat anti-mouse-FITC-conjugated secondary antibodies (Invitrogen). The whole mount staining of the poplar and *Arabidopsis* root hairs with CBM3a was conducted as described previously (Park et al., 2011). Negative controls were carried out in the absence of primary antibody. Immunofluorescence was observed with an Olympus BX-51 microscope equipped with epifluorescence optics.

Crystalline cellulose content assay and glycosyl residue composition analysis

Crude cell wall preparations (alcohol-insoluble residue, AIR) were generated from 7-day-old etiolated seedlings as described previously (Cavalier et al., 2008). Crystalline cellulose content was determined using the method as described previously (Foster

et al., 2010). Briefly, 1 mg of cell wall AIRs were hydrolyzed by trifluoroacetic acid (TFA) at 120 °C for 120 min. The TFA-resistant materials were treated with Updegraff reagent (acetic acid: nitric acid: water, 8:1:2, v/v) at 100 °C for 30 min, and the resulting pellets were then completely hydrolyzed with 67% H₂SO₄ (v/v). The released glucose was measured using a glucose assay kit (Cayman Chemical, MI) using a dehydration factor of 0.9.

Monosaccharide composition analysis was performed with TFA-hydrolyzed materials as described previously (Yu et al., 2010). The released monosaccharides were derived by 1-phenyl-3-methyl-5-pyrazolone (PMP) and the derivatives were analyzed by HPLC.

Results

PdCSLD5 and *PdCSLD6* are strongly expressed in root, including in the root hairs

Two poplar genes named *CSLD5* and *CSLD6* were predicted from the *Populus trichocarpa* genome database based on the sequence similarity to the *Arabidopsis AtCSLD3/KOJAK* gene (Suzuki et al., 2006; Dharmawardhana et al., 2010), which is further confirmed by phylogenetic analysis of the *Populus* and *Arabidopsis* *CSLD* subfamily (Fig. 1A). Except the *Populus trichocarpa* sequences used for bioinformatic analyses, all the sequences of poplar *CSLD5* and *CSLD6* mentioned in this paper are from *Populus deltoides*. As a first step toward the molecular characterization, we isolated the corresponding genes, *PdCSLD5* and *PdCSLD6*, by screening a root cDNA library of *Populus deltoides*. The longest open reading frames of *PdCSLD5* and *PdCSLD6* both have 3432 nucleotides, and encode a putative protein of 1143 amino acid residues with different predicted molecular mass (128,267 Da and 128,070 Da) and pI (7.55 and 7.44). Pairwise comparisons of the deduced amino acid sequences showed that *PdCSLD5* and *PdCSLD6* both exhibit 86% identities to *AtCSLD3* (Fig. 1B). A Pfam search showed that each protein has a D.D.D_QxxRW motif (Fig. 1B) and belongs to GT family 2 (Cantarel et al., 2009), indicating that they might be involved in the synthesis of β-linked glycan. Synteny analysis showed that *PdCSLD5* and *PdCSLD6* were duplicated genes derived from segmental duplications during the evolutionary process (Fig. 1C).

Next we examined the expression patterns of *PdCSLD5* and *PdCSLD6* in different tissues of poplar using qRT-PCR. Although *PdCSLD5* and *PdCSLD6* were ubiquitously expressed in various tissues examined, their highest transcript accumulations were observed in young roots (Fig. 2A). To explore more detailed expression patterns of *PdCSLD5* and *PdCSLD6*, we then performed *in situ* hybridization to examine their expressions in poplar roots. The *PdCSLD5* and *PdCSLD6* hybridization signals were observed in cortex, epidermis and protoxylem cells, including in the root hairs (Fig. 2B and C). The controls hybridized with the sense probes did not show signals in roots.

We also generated transgenic *Arabidopsis* plants harboring the *PdCSLD5* or *PdCSLD6* putative promoter region fused with the *GUS* gene to verify the conservation of expression patterns of *PdCSLD5* or *PdCSLD6* versus *AtCSLD3*. As shown in Supplementary Fig. S1, although *GUS* was expressed ubiquitously in all tissues examined, the most intensive signals were present in roots, including in the root hairs, which is consistent with the expression pattern of *AtCSLD3* in *Arabidopsis* (Favery et al., 2001; Wang et al., 2001). These results indicate that the cis-elements in the promoters of *PdCSLD5*, *PdCSLD6* and *AtCSLD3* were highly conserved.

Supplementary data associated with this article can be found, in the online version, at <http://dx.doi.org/10.1016/j.jplph.2013.04.014>.

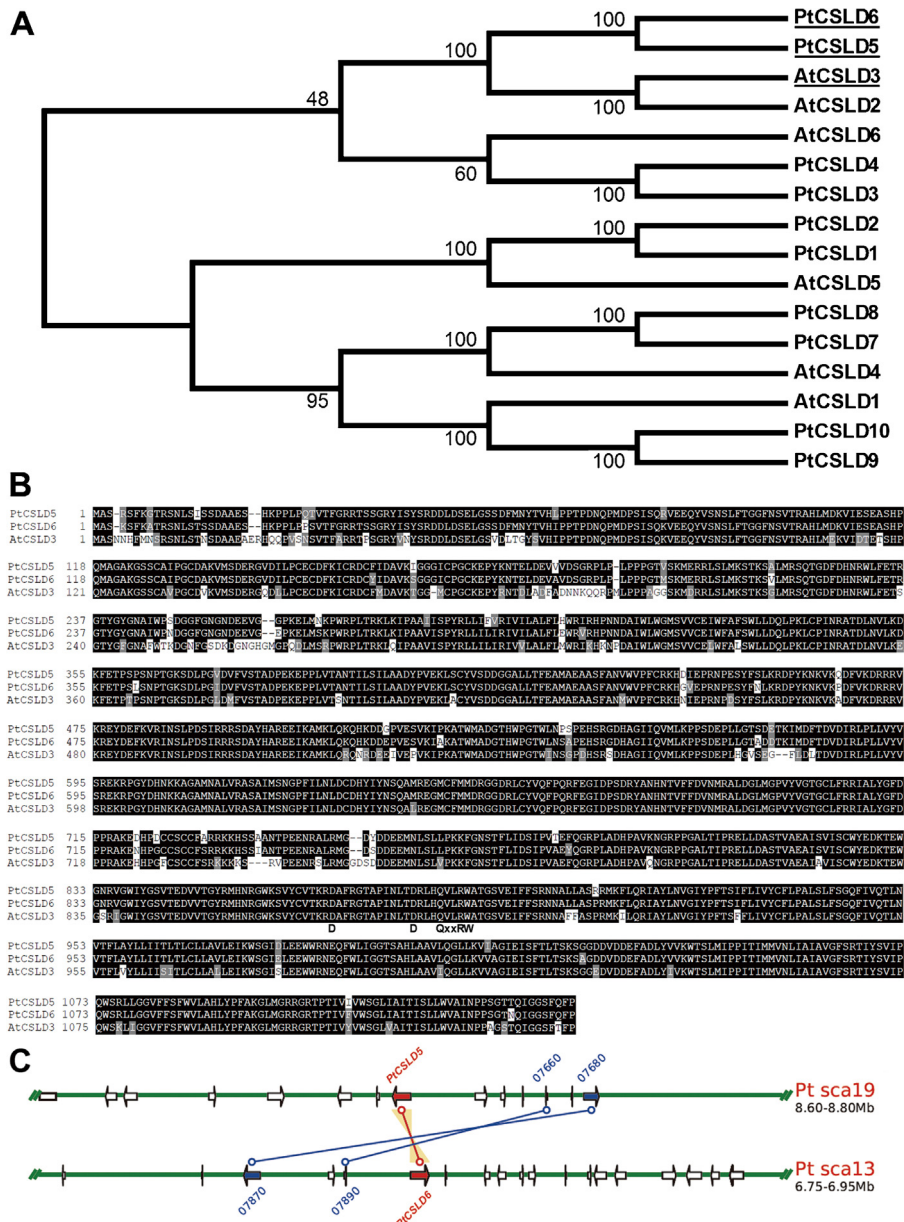


Fig. 1. Bioinformatic analysis of PdCSLD5 and PdCSLD6 (A) Joined phylogenetic tree of CSDL members in *Populus trichocarpa* and *Arabidopsis* constructed with MEGA 4.0 by the Neighbor-Joining (NJ) method with 1000 bootstrap replicates. (B) Amino acid sequence alignment of PdCSLD5 and PdCSLD6 from *Populus deltoides* and AtCSLD3/KOJAK. The numbers shown at the left of each sequence are the positions of amino acid residues in the corresponding proteins. Gaps (marked with dashes) were introduced to maximize the sequence alignment. Identical and similar amino acid residues are shaded with black and gray, respectively. The D.D-D.QxxRW conserved motif is indicated. (C) Segmental duplication analysis of PtCSLD5 and PtCSLD6. The blocks for PtCSLD5 and PtCSLD6 display ± 100 kb region. Blue arrows are other anchor genes in the region, PtCSLD5 and PtCSLD6 are marked in red. (For interpretation of the references to color in this figure legend, the reader is referred to the web version of the article.)

PdCSLD5 and *PdCSLD6* are targeted not only to the apical plasma membranes in root hair cells but to the Golgi apparatus in root hair and non-hair-forming epidermal cells

AtCSLD3 was shown to be localized in the Golgi apparatus (Bernal et al., 2007), and further demonstrated to be localized to the apical plasma membranes at the root hairs tips as well (Park et al., 2011), which is in agreement with its proposed role in root hair formation. To investigate whether PdCSLD5 and PdCSLD6 play roles similar to AtCSLD3, the subcellular locations were studied. Both PdCSLD5 and PdCSLD6 are predicted to be type II membrane proteins that contain 8 transmembrane helices, a non-cytoplasmic N-terminus, a second non-cytoplasmic region located between the second and the third transmembrane helices, and

a short non-cytoplasmic C-terminal region (Fig. 3A and B). PdCSLD5 and PdCSLD6 were tagged with GFP at the N-terminus and expressed in *Arabidopsis*, respectively. The same as the previous report of AtCSLD3 localization (Park et al., 2011), confocal imaging of the GFP signals in root cells of 4-day-old transgenic seedlings showed that both GFP-PdCSLD5 (Fig. 3C) and GFP-PdCSLD6 (Fig. 3G) were co-localized with the membrane-selective dye FM4-64 labeling (Fig. 3D and H) to the apical cell peripheries of the root hairs, and exhibited a punctate pattern in the cytoplasm of non-hair-forming epidermal cells (Fig. 3K and O). Interestingly, they were also found to exhibit a punctate pattern in the basal region of the root hairs (Fig. 3C-E and G-I), suggesting certain organelles localization out of the extreme tip of the root hairs.

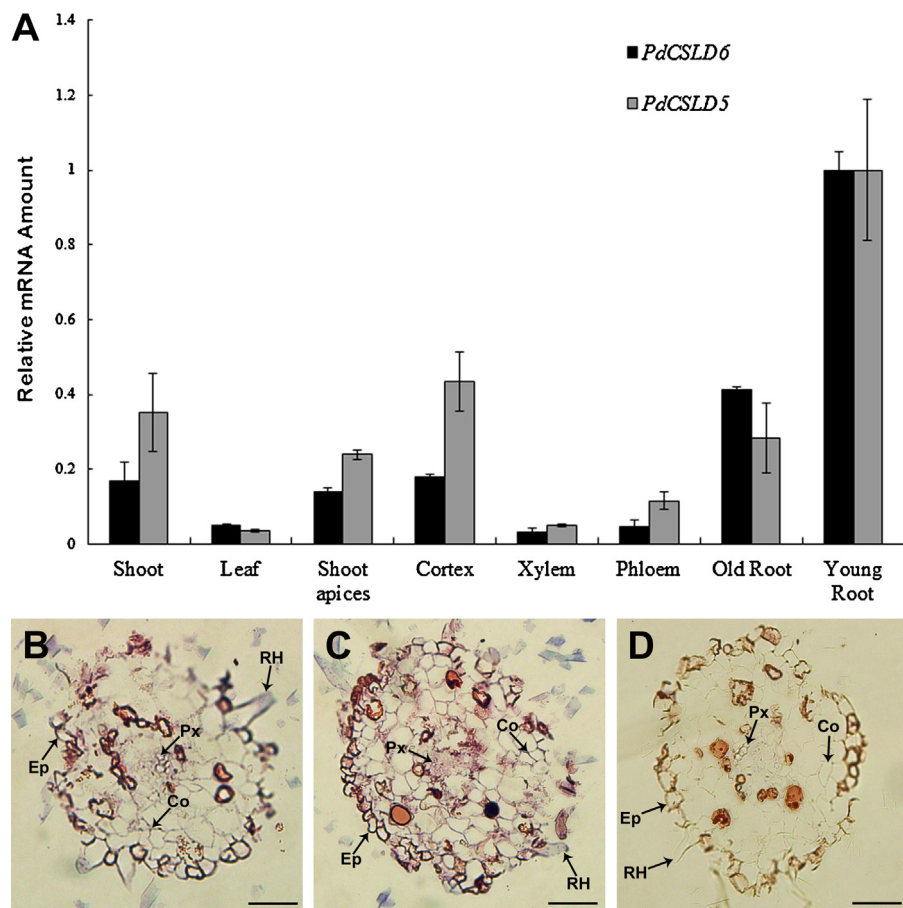


Fig. 2. Expression Analysis of *PdCSLD5* and *PdCSLD6* Using qRT-PCR and *in situ* Hybridization. (A) qRT-PCR detection of the expression of *PdCSLD5* and *PdCSLD6* in poplar. The relative mRNA abundance of *PdCSLD5* and *PdCSLD6* in all samples was normalized with respect to reference gene *UBQ10* in different tissues and the *PdCSLD5* and *PdCSLD6* expression levels in young root are set to 1. The bars are standard deviations (SD) of three biological replicates. (B-D) *In situ* hybridization detection of the expression of *PdCSLD5* and *PdCSLD6* in poplar roots. Cross-sections of roots were hybridized with the digoxigenin-labeled antisense *PdCSLD5* (B) and *PdCSLD6* (C) RNA probes or sense *PdCSLD5* RNA probe (D), and the hybridization signals were detected by alkaline phosphatase-conjugated antibodies and are shown in purple or blue. (B, C) Cross-section of roots showing the *PdCSLD5* (B) and *PdCSLD6* (C) signals in the cortex, epidermis and protoxylem cells, including in the root hairs. (D) A control root section hybridized with the sense *PdCSLD5* probe showing the absence of hybridization signals. Co, cortex; Ep, epidermis; Px, protoxylem; RH, root hair. Scale bars represent 50 μ m. (For interpretation of the references to color in this figure legend, the reader is referred to the web version of the article.)

To further determine the organelles in root hair and non-hair-forming epidermal cells that *PdCSLD5* and *PdCSLD6* located in, GFP-*PdCSLD5* and GFP-*PdCSLD6* were co-transfected with the Golgi marker Man49-mCherry (Nelson et al., 2007), into *Nicotiana benthamiana* leaves, respectively. Both GFP-*PdCSLD5* (Fig. 3L–N) and GFP-*PdCSLD6* (Fig. 3P–R) signals were demonstrated to be co-localized with the Man49-mCherry, suggesting that *PdCSLD5* and *PdCSLD6* are also targeted to the Golgi apparatus. Taken together, localization experiments revealed that *PdCSLD5* and *PdCSLD6* are targeted not only to the apical plasma membranes in root hair cells but to the Golgi apparatus in root hair and non-hair-forming epidermal cells.

PdCSLD5 and *PdCSLD6* rescue the *atcsld3* mutant phenotypes

To test whether *PdCSLD5* and *PdCSLD6* are functionally conserved with *AtCSLD3*, their abilities to rescue the *atcsld3* mutant defects were examined. The full-length *PdCSLD5* and *PdCSLD6* cDNAs driven by the CaMV 35S promoter were expressed in the *atcsld3* mutant, respectively. Transgenic lines were tested for the presence of *PdCSLD5* and *PdCSLD6* transgenes in a homozygous *atcsld3* background. RT-PCR analysis confirmed the expression of the *PdCSLD5* and *PdCSLD6* transcript in these lines (Data not shown).

The *atcsld3* mutant showed defective root hair growth that root hairs rupture at their tips soon after initiation (Favery et al., 2001;

Wang et al., 2001). Expression of either *PdCSLD5* or *PdCSLD6* in *atcsld3* can restore the morphological defects of root hairs (Fig. 4A). In fact, the root hair morphology of the complemented lines is indistinguishable from that of WT. Interestingly, the *PdCSLD6*-complemented plants produced longer root hairs compared to WT (Fig. 4A and B), and the root hair density also increases slightly (Fig. 4C). It is noteworthy that the length of root hairs is only partially restored in the *PdCSLD5*-complemented lines (Fig. 4A and B). This observation indicated that the rescuing ability of *PdCSLD5* is relatively weaker compared to *PdCSLD6* although their encoding proteins share 94% sequence identity (Fig. 1B), which suggested that there may be partial redundancy in their function in the root hair formation.

PdCSLD5 and *PdCSLD6* restore the deficiency of crystalline cellulose in *atcsld3*

Previous research supports a role for *AtCSLD3* in the synthesis of cellulose or a cellulose-like (1 → 4)- β -glucan polysaccharides in the apical plasma membranes of root hair cells (Park et al., 2011). To further gain insights into the specific function of CSLDs during the root hair formation and demonstrate whether the morphological complementation by *PdCSLD5* and *PdCSLD6* could be correlated with the rescue of cell wall polysaccharides synthesis, we first analyzed the glycosyl residue compositions of root cell

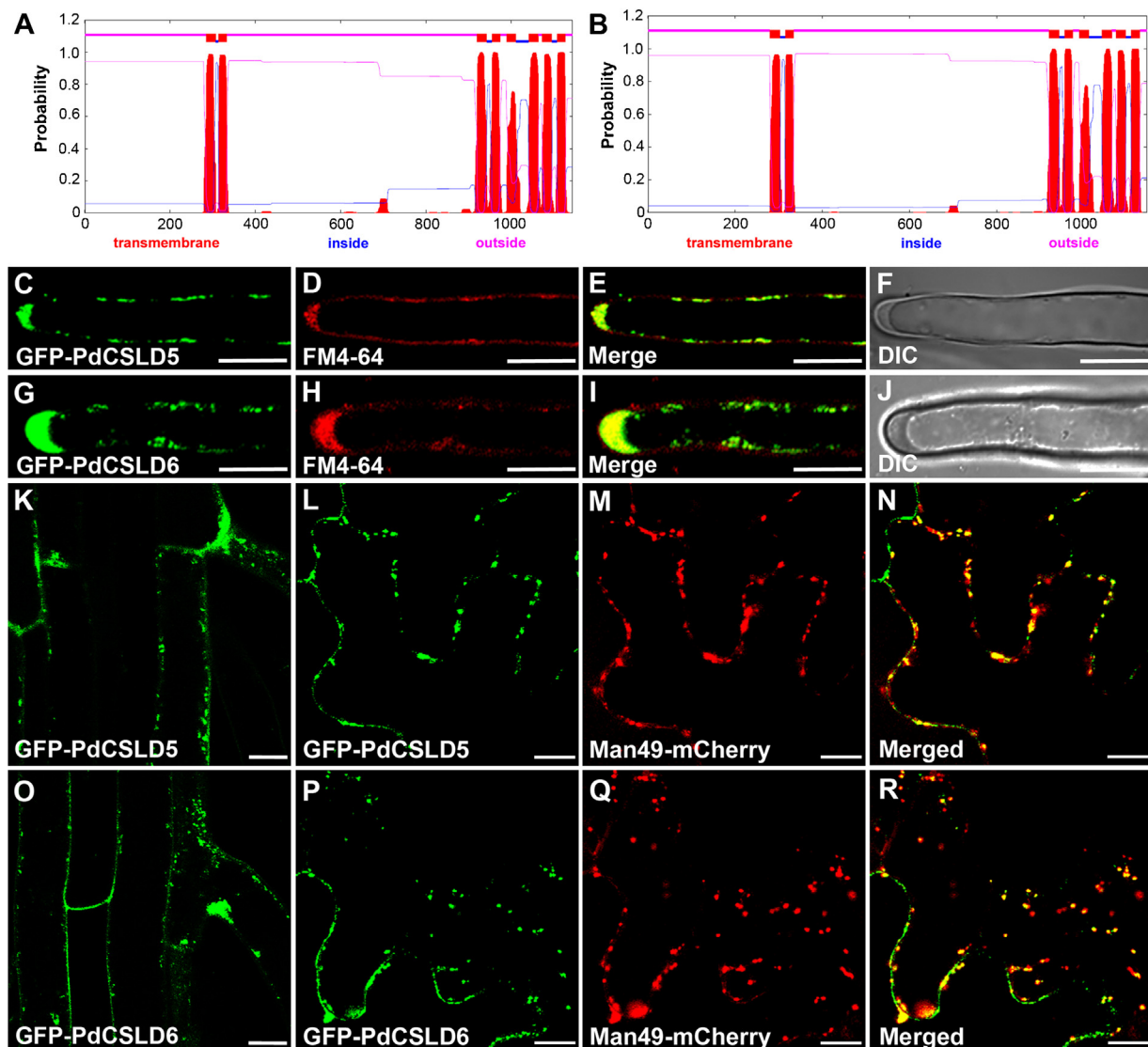


Fig. 3. Subcellular localization of GFP tagged PdCSLD5 and PdCSLD6. GFP tagged PdCSLD5 and PdCSLD6 were expressed in *Arabidopsis* and *Nicotiana benthamiana* plants, and their fluorescence signals were visualized using a laser confocal microscope. Scale bars represent 10 μm . (A, B) PdCSLD5 and PdCSLD6 are type II membrane protein predicted by the TMHMM2.0 program. (C–F, G–J) Root hair cells of 4-day-old *Arabidopsis* seedlings stably expressing GFP-PdCSLD5 (C) or GFP-PdCSLD6 (G) stained with the membrane-selective dye FM4-64 (D, H), with a merged image (E, I) and DIC image (F, J). Note the superimposition of GFP-PdCSLD5 or GFP-PdCSLD6 with FM4-64 signals at the root hair tips. (K, O) Root cells of 4-day-old *Arabidopsis* seedlings stably expressing GFP-PdCSLD5 (K) or GFP-PdCSLD6 (O), showing their punctate pattern in non-hair-forming epidermal cells and the basal region of the root hairs. (L–N, P–R) Tobacco leaf epidermal cells co-expressing GFP-PdCSLD5 (L) or GFP-PdCSLD6 (P) with Golgi marker Man49-mCherry (M, Q) with a merged image (N, R), showing co-localization of GFP-PdCSLD5 or GFP-PdCSLD6 with Man49-mCherry.

walls of WT, *atcsld3* and the transgenic plants. Crude cell wall preparations (alcohol-insoluble residue, AIR) from 7-day-old etiolated seedlings were hydrolyzed with trifluoroacetic acid (TFA), which can release monosaccharides from non-cellulosic polysaccharides and non-crystalline β -1,4-glucan (Cavalier et al., 2008). As indicated in Table 1, the amount of glucose in *atcsld3* was remarkably increased by about 84% compared with that of WT,

whereas the amount of xylose and fucose, representing xyloglucan (Cavalier et al., 2008), was not altered significantly, which suggested that the increased glucose level in *atcsld3* may largely result from the increased non-crystalline β -1,4-glucan, rather than xyloglucan. Overexpression of either PdCSLD5 or PdCSLD6 in *atcsld3* restored the level of glucose to 145% and 118% of the WT level, respectively. We also determined the total amount of crystalline

Table 1

Glycosyl residue composition analysis of cell wall residues isolated from WT, *atcsld3*, PdCSLD5-complemented and PdCSLD6-complemented plants.

Sample	Man	Rha	GlcA	GalA	Glc	Gal	Xyl	Ara	Fuc
WT	1.85 ± 0.1	5.95 ± 0.7	0.97 ± 0.1	15.88 ± 0.2	15.5 ± 0.1	27.23 ± 0.6	10.77 ± 0.6	16.05 ± 0.2	1.77 ± 0.2
<i>atcsld3</i>	1.83 ± 0.2	3.6 ± 0.1*	0.51 ± 0.2*	14.34 ± 0.9	28.52 ± 0.5*	21.72 ± 0.3*	11.32 ± 0.3	13.32 ± 0.2	1.55 ± 0.1
<i>atcsld3</i> +PdCSLD5	1.71 ± 0.2	4.60 ± 0.6*	0.45 ± 0.2*	14.89 ± 0.1	22.47 ± 1.7*	27.11 ± 1.5	10.61 ± 0.1	15.31 ± 0.3	1.56 ± 0.1
<i>atcsld3</i> +PdCSLD6	1.82 ± 0.1	6.10 ± 0.5	0.41 ± 0.3*	16.25 ± 1.2	18.28 ± 2.4	25.88 ± 1.0	11.59 ± 1.5	15.48 ± 0.4	1.67 ± 0.05

Cell wall residues were generated from 7-day-old etiolated seedlings of *Arabidopsis* WT, *atcsld3*, PdCSLD5-complemented (*atcsld3*+PdCSLD5) and PdCSLD6-complemented (*atcsld3*+PdCSLD6) *atcsld3* seedlings. The results are given as means ($\mu\text{g mg}^{-1}$ of AIR) of three biological replicates.

* Significance between WT and mutant or complemented seedlings determined by the least-significant difference (t test at $P < 0.05$).

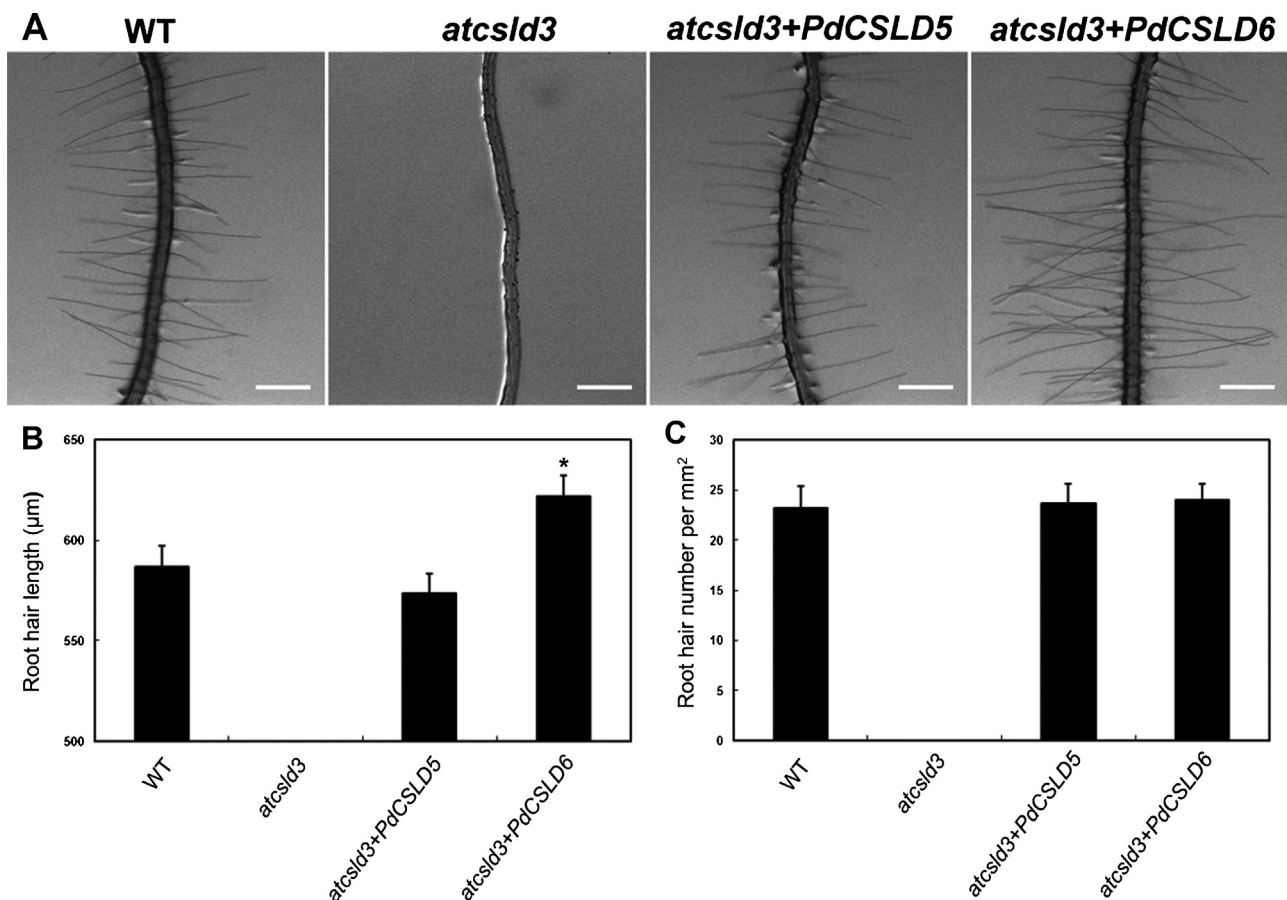


Fig. 4. Complementation analysis of root hair phenotypes in *atcsl3* plants by overexpression of *PdCSLD5* or *PdCSLD6*. All seedlings were grown under the same conditions on vertical agar plates for 7 d. For root hair length and density analysis, 192 fully elongated root hairs were measured (n roots = 24). Values are means \pm SD. (A) Root hair phenotypes of *atcsl3*, WT, *PdCSLD5*-complemented and *PdCSLD6*-complemented *atcsl3* lines. (B, C) Root hair length (B) and density (C) analysis of *atcsl3*, WT, *PdCSLD5*-complemented and *PdCSLD6*-complemented *atcsl3* seedlings. Root hair density is shown as root hair number per mm^2 .

cellulose of the root cell walls. Noticeably, the crystalline cellulose content was decreased by about 30% in *atcsl3* compared to WT, which was largely restored to 90% and 104% of WT level in *PdCSLD5* and *PdCSLD6* complemented *atcsl3* lines, respectively (Fig. 5).

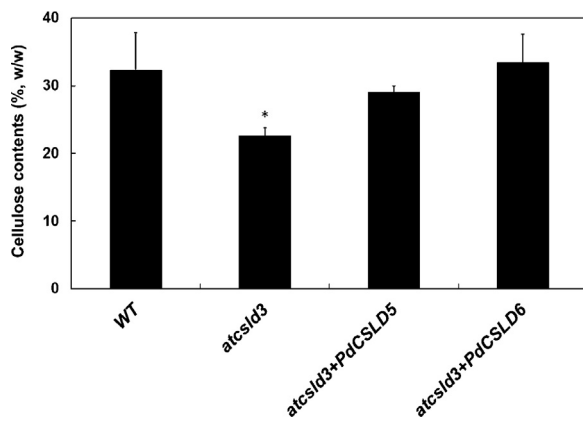


Fig. 5. Crystalline cellulose content analysis of *Arabidopsis* WT, *atcsl3*, *PdCSLD5*-complemented and *PdCSLD6*-complemented *atcsl3* lines. Cell wall residues were generated from 7-day-old etiolated *Arabidopsis* seedlings. The crystalline cellulose content was determined by the Updegraff method. The results presented are the weight percentage (w/w). Each data point represents the mean of three biological replicates. *Significance determined by the least-significant difference (t test at $P < 0.05$).

To further confirm the above results, we first performed immunohistochemical analysis in the cross-sections of 4-day-old *Arabidopsis* roots using a series of monoclonal antibodies and carbohydrate-binding modules (CBMs). These probes included monoclonal antibodies CCRC-M1, CCRC-M88 and CCRC-M101 directed against xyloglucan (Cavalier et al., 2008), LM10 and LM11 against xylan (McCartney et al., 2005), and CBM3a and CBM17 to crystalline cellulose and non-crystalline β -1,4-glucan, respectively (Blake et al., 2006). Immunolabeling of cross-sections of 4-day-old WT roots with CBM3a showed strong binding in pericycle, epidermis, cortex and endodermis cells (Fig. 6A2). However, less labeling was observed in all *atcsl3* root walls except cortex compared to WT (Fig. 6A1). Conversely, a relatively strong CBM17 labeling was observed in *atcsl3* root cells compared to that of WT (Fig. 6B1 and B2). In *PdCSLD5* or *PdCSLD6* complemented *atcsl3* lines, CBM3a and CBM17 labeling were mostly restored to the WT levels (Fig. 6A3, A4, B3 and B4). Besides, no significant differences were detected in either labeling intensity or patterns of the xyloglucan and xylan directed antibodies (Fig. 6C1–G4). Then, we performed whole mount staining with CBM3a in the root hairs of 4-day-old *Arabidopsis* seedlings, and strong binding was observed in the growing root hair tips of WT, while the labeling level of the two transgenic lines were mostly restored to that of WT (Supplementary Fig. S2).

Supplementary data associated with this article can be found, in the online version, at <http://dx.doi.org/10.1016/j.jplph.2013.04.014>.

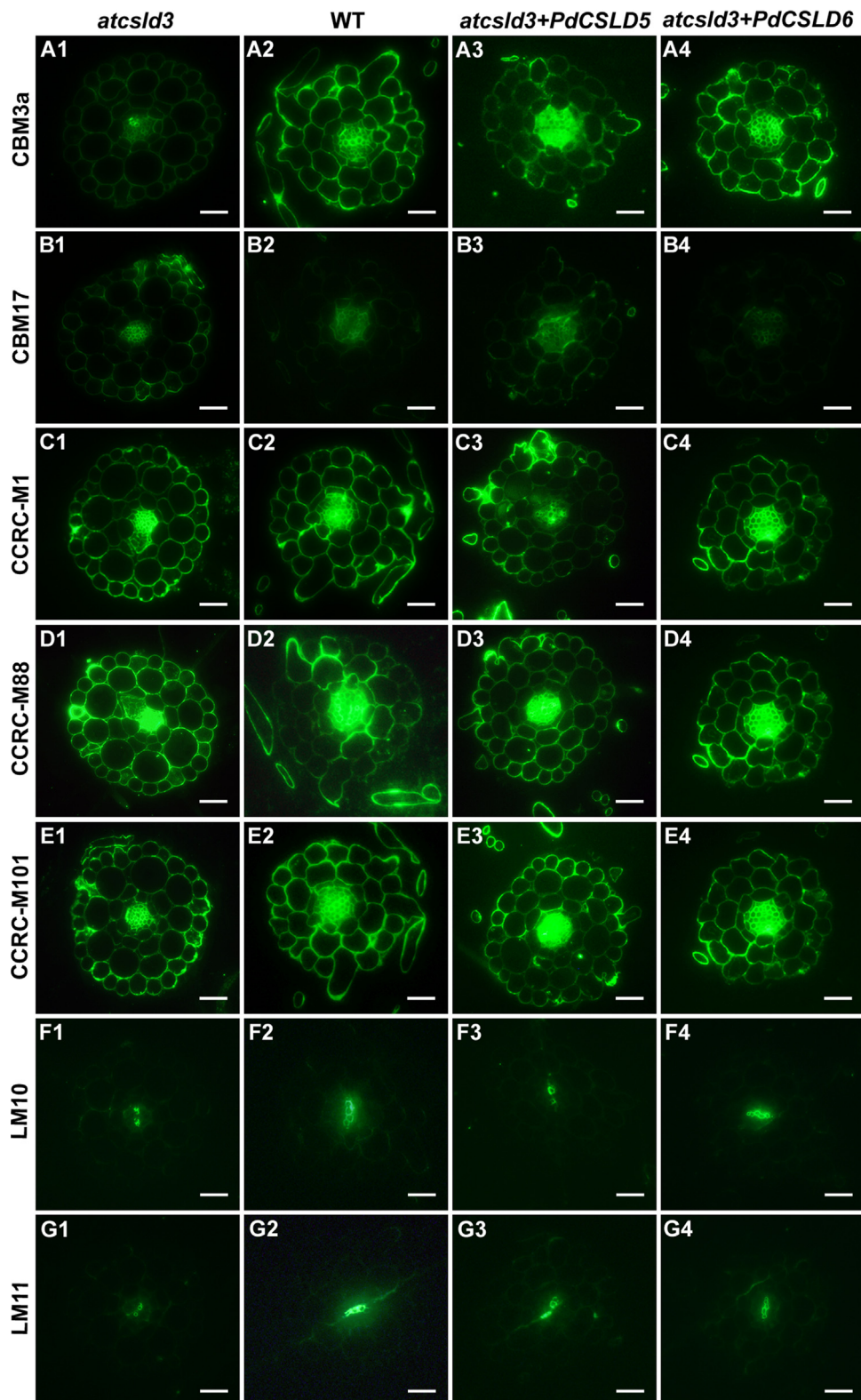


Fig. 6. Immunolocalization of transverse sections of *atclsd3*, WT, *PdCSLD5*-complemented and *PdCSLD6*-complemented *atclsd3* roots. (A1–A4) *atclsd3*, WT, *PdCSLD5*-complemented and *PdCSLD6*-complemented *atclsd3* plants labeled with CBM3a. (B1–B4) *atclsd3*, WT, *PdCSLD5*-complemented and *PdCSLD6*-complemented *atclsd3* plants labeled with CBM17. (C1–E4) *atclsd3*, WT, *PdCSLD5*-complemented and *PdCSLD6*-complemented *atclsd3* plants labeled with CCRC-M1, CCRC-M88 and CCRC-M101. (F1–G4) *atclsd3*, WT, *PdCSLD5*-complemented and *PdCSLD6*-complemented *atclsd3* plants labeled with LM10 and LM11.

Discussion

CSLD proteins were proposed to synthesize polysaccharides that have specialized structural roles in the cell walls of root hair cells

and other tip-growing cells (Bernal et al., 2008). Therefore, studying the roles of specific CSLD genes will provide a better understanding to the molecular mechanism of the root hair formation and plant cell tip growth. However, little is known about the genes

involved in the root hair development in dicot wood species. In this study, two poplar genes, *PdCSLD5* and *PdCSLD6*, were identified from *Populus deltoids*. The results from complementation and cell wall polysaccharide composition analysis supported a specialized role for *PdCSLD5* and *PdCSLD6* in root hair formation and crystalline cellulose production at the root hair tips in poplar.

Expression analysis showed that *PdCSLD5* and *PdCSLD6* are strongly expressed in the root cells, including in the root hairs, although their transcripts are detected in all tissues examined (Fig. 2), and the *atcsls3* phenotype was shown to be restricted to the root hairs while *AtCSLD3* is expressed in all tissues (Favery et al., 2001; Wang et al., 2001). We have demonstrated that overexpression of either *PdCSLD5* or *PdCSLD6* can compensate most of the root hair defects caused by the *AtCSLD3* mutation (Fig. 4A), indicating that these two poplar genes are functionally conserved with *AtCSLD3*. In addition, previous research showed that there is partial redundancy of *AtCSLD2* and *AtCSLD3* during root hair formation (Bernal et al., 2008). *AtCSLD2* and *AtCSLD3* share 89% identity to each other, and *PdCSLD5* and *PdCSLD6* both exhibit 85% identities to *AtCSLD2* (while both of them share 86% identities to *AtCSLD3*). Considering the high identities of *PdCSLD5* and *PdCSLD6* to *AtCSLD2*, it is hard to get rid of the possibility that *PdCSLD5* and/or *PdCSLD6* be the homolog(s) of *AtCSLD2*. To confirm this assumption, it is necessary to further examine the abilities of *PdCSLD5* and *PdCSLD6* to rescue the defects of *atcsls2* mutant in the future study.

In the present work, the *PdCSLD6*-complemented *atcsls3* plants produced longer root hairs compared to WT plants, while the length of root hairs is only partially restored in the *PdCSLD5*-complemented *atcsls3* lines (Fig. 4A and B). This observation showed that the rescuing ability of *PdCSLD5* is weaker in comparison to *PdCSLD6*, which suggested that there is partial functional redundancy of these two genes during root hair formation. Previous studies revealed that the segmental duplication associated with the salicoid duplication event contributed remarkably to the expansion of many multi-gene families in *Populus* genome (Hu et al., 2010, 2012; Barakat et al., 2011). Synteny analysis indicated that *PdCSLD5* and *PdCSLD6* were segmental duplicated genes (Fig. 1C). According to the duplication–degeneration–complementation model (Force et al., 1999), most duplicated genes accumulate degenerative mutations for a certain time after the duplication event and then undergo functional specialization by complementary partitioning of the functions of the ancestral gene. The differences in the rescuing ability observed for *PdCSLD5* and *PdCSLD6* suggest that this type of sub-functionalization may have occurred in these two poplar genes during subsequent evolutionary process.

It is interesting to note that the abilities of *PdCSLD5* and *PdCSLD6* for rescuing the *atcsls3* root hair defect are further confirmed to be correlated with the rescue of crystalline cellulose synthesis. As indicated in Fig. 5, the deficiency of crystalline cellulose in the *atcsls3* roots was completely restored in the *PdCSLD6*-complemented *atcsls3* plants, while only partially rescued in the *PdCSLD5*-complemented plants. Interestingly, the total amount of glucose in *atcsls3* was remarkably increased by about 84% compared to that of the WT. However, the amount of xylose and fucose, representing xyloglucan (Cavalier et al., 2008), was hardly altered in *atcsls3*, suggesting that the increased glucose level in *atcsls3* may largely result from the increased non-crystalline β -1,4-glucan, rather than xyloglucan. These observations were further proved by immunohistochemical analysis in both the root hair and the root cross-sections of 4-day-old *Arabidopsis* seedlings (Fig. 6, Supplementary Fig. S2). To provide further support for the role of *PdCSLD5* and *PdCSLD6* in cellulose synthesis in poplar root hairs, we also stained poplar root hair cells with CBM3a, and a strong binding was observed in the growing root hair tips, indicating the presence of high abundance of cellulose wherein (Supplementary Fig. S3). Taken together, these results provide support for a specific role of

PdCSLD5 and *PdCSLD6* in crystalline cellulose biosynthesis in poplar root hairs.

Supplementary data associated with this article can be found, in the online version, at <http://dx.doi.org/10.1016/j.jplph.2013.04.014>.

Subcellular localization experiments showed that *PdCSLD5* and *PdCSLD6* are localized in the polarized plasma membrane in root hair and the Golgi apparatus of the non-hair-forming cells (Fig. 3), which is consistent with previous reports of *AtCSLD3* localization (Park et al., 2011). It is noteworthy that *PdCSLD5* and *PdCSLD6* were also localized in the Golgi apparatus in the sub-apical regions and the basal region of root hairs (Fig. 3K and O). Furthermore, the dual subcellular localization pattern observed in these CSLDs was also found in the process of assemblage of CESA complexes, in which the inactive form of CESA proteins were first recruited into CESA rosette complexes in the Golgi apparatus, and then the rosette complexes were exocytosed to plasma membrane where CESAs become activated (Somerville, 2006). Although how the CESAs (or CSLDs) had been activated remains to be elucidated, the similar dual localization pattern supports the probable function of *PdCSLD5* and *PdCSLD6* as cellulose synthase in polarized plasma membrane of root hairs.

Previous studies indicated that the cellulose synthases function in the form of organized rosette complexes composed of at least three different CESAs (Taylor et al., 2003; Desprez et al., 2007), and other than CESAs, CSLDs are the only members of the CSLs that have the N-terminal zinc finger-like domain that was thought to function in protein–protein interactions, possibly mediating the formation of complexes or protein turnover (Richmond and Somerville, 2000; Gamsjaeger et al., 2007). In addition, so far, there is no report for the CESAs to be essential for cellulose synthesis in tip-growing root hairs (Caño-Delgado et al., 2003; Singh et al., 2008), suggesting that GTs that are not classified within the CESA family could contribute to cellulose synthesis in tip-growing root hairs. Combined with the present results and previous reports, it can be speculated that *PdCSLD5* and *PdCSLD6* may function in a similar fashion as CESAs by serving as an individual synthase monomer to form complexes with other proteins to be involved in cellulose synthesis at the root hair tips. Consequently, one explanation of these cellulose and glucose content alterations is that the β -1,4-glucan chains synthesized by other synthase monomers in *atcsls3* were accumulated in a non-crystalline form, thus leading to an increase of non-crystalline β -1,4-glucan content and a decrease of cellulose content. Similarly, based on the above postulation, *PdCSLD5* and *PdCSLD6* can functionally replace *AtCSLD3* to form cellulose–synthase complexes to participate in cellulose synthesis at the root hair tips, thus leading to restoration of cellulose content and a decrease in non-crystalline β -1,4-glucan content in the complemented lines.

In conclusion, our data provide evidences demonstrating that *PdCSLD5* and *PdCSLD6* are functionally conserved with *AtCSLD3* and support a specific role for *PdCSLD5* and *PdCSLD6* in crystalline cellulose production in poplar root hairs, which would help us gain new insights into the mechanism underlying the crystalline cellulose synthesis. Besides, *PdCSLD5* and *PdCSLD6* may be a platform for not only understanding root hair development in dicot wood but also for launching comparative studies between different species.

Acknowledgements

This study was supported by grants from the National Basic Research Program of China (2012CB114501), the National Natural Science Foundation of China (Nos. 30901157, 31070272 and 31000311), the Program of 100 Distinguished Young Scientists of the Chinese Academy of Sciences (to Gongke Zhou), the National High-Tech Research and Development Program of China

(2009AA10Z101 and 2011AA100209) and the Promotive Research Fund for young and middle-aged scientists of Shandong Province (BS2011SW055). We would like to thank Dr. Michael G. Hahn (Complex Carbohydrate Research Center, University of Georgia, USA) and Dr. J. Paul Knox (Center for Plant Sciences, Faculty of Biological Sciences, University of Leeds, United Kingdom) for the antibodies and CBMs.

References

- Barakat A, Choi A, Yassin NB, Park JS, Sun Z, Carlson JE. Comparative genomics and evolutionary analyses of the O-methyltransferase gene family in *Populus*. *Gene* 2011;479:37–46.
- Bernal AJ, Jensen JK, Harholt J, Sorensen S, Moller I, Blaukopf C, et al. Disruption of ATCSLD5 results in reduced growth, reduced xylan and homogalacturonan synthase activity and altered xylan occurrence in *Arabidopsis*. *Plant J* 2007;52:791–802.
- Bernal AJ, Yoo CM, Mutwil M, Jensen JK, Hou G, Blaukopf C, et al. Functional analysis of the cellulose synthase-like genes CSLD1, CSLD2, and CSLD4 in tip-growing *Arabidopsis* cells. *Plant Physiol* 2008;148:1238–53.
- Blake AW, McCartney L, Flint JE, Bolam DN, Boraston AB, Gilbert HJ, et al. Understanding the biological rationale for the diversity of cellulose-directed carbohydrate-binding modules in prokaryotic enzymes. *J Biol Chem* 2006;281:29321–9.
- Burton RA, Jobling SA, Harvey AJ, Shirley NJ, Mather DE, Bacic A, et al. The genetics and transcriptional profiles of the cellulose synthase-like HvCslF gene family in barley. *Plant Physiol* 2008;146:1821–33.
- Burton RA, Wilson SM, Hrmova M, Harvey AJ, Shirley NJ, Medhurst A, et al. Cellulose synthase-like CslF genes mediate the synthesis of cell wall (1,3;1,4)-beta-D-glucans. *Science* 2006;311:1940–2.
- Caño-Delgado A, Penfield S, Smith C, Catley M, Bevan M. Reduced cellulose synthesis invokes lignification and defense responses in *Arabidopsis thaliana*. *Plant J* 2003;34:351–62.
- Cantarel BL, Coutinho PM, Rancurel C, Bernard T, Lombard V, Henrissat B. The carbohydrate-active enzymes database (CAZy): an expert resource for glycogenomics. *Nucleic Acids Res* 2009;37:D233–8.
- Carol RJ, Dolan L. Building a hair: tip growth in *Arabidopsis thaliana* root hairs. *Philos Trans R Soc Lond B Biol Sci* 2002;357:815–21.
- Cavalier DM, Lerouxel O, Neumetzler L, Yamauchi K, Reinecke A, Freshour G, et al. Disrupting two *Arabidopsis thaliana* xylosyltransferase genes results in plants deficient in xyloglucan, a major primary cell wall component. *Plant Cell* 2008;20:1519–37.
- Chen QJ, Zhou HM, Chen J, Wang XC. Using a modified TA cloning method to create entry clones. *Anal Biochem* 2006;358:120–5.
- Cocuron JC, Lerouxel O, Drakakaki G, Alonso AP, Liepmann AH, Keegstra K, et al. A gene from the cellulose synthase-like C family encodes a beta-1,4 glucan synthase. *Proc Natl Acad Sci U S A* 2007;104:8550–5.
- Desprez T, Juranić M, Crowell EF, Jouy H, Pochylova Z, Parcy F, et al. Organization of cellulose synthase complexes involved in primary cell wall synthesis in *Arabidopsis thaliana*. *Proc Natl Acad Sci U S A* 2007;104:15572–7.
- Dharmawardhana P, Brunner AM, Strauss SH. Genome-wide transcriptome analysis of the transition from primary to secondary stem development in *Populus trichocarpa*. *BMC Genom* 2010;11:150.
- Dhugga KS, Barreiro R, Whitten B, Stecca K, Hazebroek J, Randhawa GS, et al. Guar seed beta-mannan synthase is a member of the cellulose synthase super gene family. *Science* 2004;303:363–6.
- Doblin MS, De Melis L, Newbiggin E, Bacic A, Read SM. Pollen tubes of *Nicotiana alata* express two genes from different beta-glucan synthase families. *Plant Physiol* 2001;125:2040–52.
- Dolan L, Duckett CM, Grierson C, Linstead P, Schneider K, Lawson E, et al. Clonal relationships and cell patterning in the root epidermis of *Arabidopsis*. *Development* 1994;120:2465–74.
- Favery B, Ryan E, Foreman J, Linstead P, Boudonck K, Steer M, et al. KOJAK encodes a cellulose synthase-like protein required for root hair cell morphogenesis in *Arabidopsis*. *Genes Dev* 2001;15:79–89.
- Fincher GB. Revolutionary times in our understanding of cell wall biosynthesis and remodeling in the grasses. *Plant Physiol* 2009;149:27–37.
- Force A, Lynch M, Pickett FB, Amores A, Yan YL, Postlethwait J. Preservation of duplicate genes by complementary, degenerative mutations. *Genetics* 1999;151:1531–45.
- Foreman J, Dolan L. Root hairs as a model system for studying plant cell growth. *Ann Bot* 2001;88:1–7.
- Foster CE, Martin TM, Pauly M. Comprehensive compositional analysis of plant cell walls (lignocellulosic biomass) part II: carbohydrates. *J Vis Exp* 2010;37:e1837.
- Galway ME. Root hair cell walls: filling in the framework. *Can J Bot* 2006;84:613–21.
- Galway ME, Eng RC, Schiefelbein JW, Wasteneys GO. Root hair-specific disruption of cellulose and xyloglucan in AtCSLD3 mutants, and factors affecting the post-rupture resumption of mutant root hair growth. *Planta* 2011;233:985–99.
- Gamsjaeger R, Liew CK, Loughlin FE, Crossley M, Mackay JP. Sticky fingers: zinc-fingers as protein-recognition motifs. *Trends Biochem Sci* 2007;32:63–70.
- Hu RB, Chi XY, Chai GH, Kong YZ, He G, Wang XY, et al. Genome-wide identification, evolutionary expansion, and expression profile of homeodomain-leucine zipper gene family in poplar (*Populus trichocarpa*). *PLoS One* 2012;7.
- Hu RB, Qi G, Kong YZ, Kong DJ, Gao Q, Zhou GK. Comprehensive analysis of NAC domain transcription factor gene family in *Populus trichocarpa*. *BMC Plant Biol* 2010;10.
- Hunter CT, Kirienko DH, Sylvester AW, Peter GF, McCarty DR, Koch KE. Cellulose synthase-like D1 is integral to normal cell division, expansion, and leaf development in maize. *Plant Physiol* 2012;158:708–24.
- Jefferson RA, Kavanagh TA, Bevan MW, Gus Fusions: Beta-glucuronidase as a sensitive and versatile gene fusion marker in higher-plants. *EMBO J* 1987;6:3901–7.
- Jelinkova K, Malinska K, Simon S, Kleine-Vehn J, Perezova M, Pejchar P, et al. Probing plant membranes with FM dyes: tracking, dragging or blocking? *Plant J* 2010;61:883–92.
- Karimi M, Inze D, Depicker A. GATEWAY(TM) vectors for Agrobacterium-mediated plant transformation. *Trends Plant Sci* 2002;7:193–5.
- Kim CM, Park SH, Il Je B, Park SH, Park SJ, Piao HL, et al. OsCSLD1, a cellulose synthase-like D1 gene, is required for root hair morphogenesis in rice. *Plant Physiol* 2007;143:1220–30.
- Lerouxel O, Cavalier DM, Liepmann AH, Keegstra K. Biosynthesis of plant cell wall polysaccharides – a complex process. *Curr Opin Plant Biol* 2006;9:621–30.
- Liepmann AH, Wilkerson CG, Keegstra K. Expression of cellulose synthase-like (Csl) genes in insect cells reveals that CslA family members encode mannan synthases. *Proc Natl Acad Sci U S A* 2005;102:2221–6.
- McCartney L, Marcus SE, Knox JP. Monoclonal antibodies to plant cell wall xylans and arabinoxylans. *J Histochem Cytochem* 2005;53:543–6.
- Nelson BK, Cai X, Nebenfuhr A. A multicolored set of in vivo organelle markers for co-localization studies in *Arabidopsis* and other plants. *Plant J* 2007;51:1126–36.
- Park S, Szumlanski AL, Gu FW, Guo F, Nielsen E. A role for CSLD3 during cell-wall synthesis in apical plasma membranes of tip-growing root-hair cells. *Nat Cell Biol* 2011;13, 973–U227.
- Persson S, Caffall KH, Freshour G, Hilley MT, Bauer S, Poindexter P, et al. The *Arabidopsis* irregular xylem8 mutant is deficient in glucuronoxylan and homogalacturonan, which are essential for secondary cell wall integrity. *Plant Cell* 2007;19:237–55.
- Peterson RL. Adaptations of root structure in relation to biotic and abiotic factors. *Can J Bot* 1992;70:661–75.
- Richmond TA, Somerville CR. The cellulose synthase superfamily. *Plant Physiol* 2000;124:495–8.
- Richmond TA, Somerville CR. Integrative approaches to determining Csl function. *Plant Mol Biol* 2001;47:131–43.
- Singh SK, Fischer U, Singh M, Grebe M, Marchant A. Insight into the early steps of root hair formation revealed by the procuste1 cellulose synthase mutant of *Arabidopsis thaliana*. *BMC Plant Biol* 2008;8.
- Somerville C. Cellulose synthesis in higher plants. *Annu Rev Cell Dev Biol* 2006;22:53–78.
- Somerville C, Bauer S, Brininstool G, Facette M, Hamann T, Milne J, et al. Toward a systems approach to understanding plant-cell walls. *Science* 2004;306:2206–11.
- Suzuki S, Li LG, Sun YH, Chiang VL. The cellulose synthase gene superfamily and biochemical functions of xylem-specific cellulose synthase-like genes in *Populus trichocarpa*. *Plant Physiol* 2006;142:1233–45.
- Tamura K, Dudley J, Nei M, Kumar S. MEGA4: Molecular evolutionary genetics analysis (MEGA) software version 4.0. *Mol Biol Evol* 2007;24:1596–9.
- Taylor NG, Howells RM, Huttly AK, Vickers K, Turner SR. Interactions among three distinct CesA proteins essential for cellulose synthesis. *Proc Natl Acad Sci U S A* 2003;100:1450–5.
- Thompson JD, Gibson TJ, Plewniak F, Jeanmougin F, Higgins DG. The CLUSTAL_X windows interface: flexible strategies for multiple sequence alignment aided by quality analysis tools. *Nucleic Acids Res* 1997;25:4876–82.
- Wang X, Cnops G, Vanderhaeghen R, De Block S, Van Montagu M, Van Lijsebettens M. AtCSLD3, a cellulose synthase-like gene important for root hair growth in *Arabidopsis*. *Plant Physiol* 2001;126:575–86.
- Yin L, Verhertbruggen Y, Oikawa A, Manisseri C, Knierim B, Prak L, et al. The cooperative activities of CSLD2, CSLD3, and CSLD5 are required for normal *Arabidopsis* development. *Mol Plant* 2011;4:1024–37.
- Yoo CM, Quan L, Blancaflor EB. Divergence and redundancy in CSLD2 and CSLD3 function during *Arabidopsis thaliana* root hair and female gametophyte development. *Front Plant Sci* 2012;3:111.
- Yu L, Zhang X, Li SS, Liu XY, Sun L, Liu HB, et al. Rhamnogalacturonan I domains from ginseng pectin. *Carbohydr Polym* 2010;79:811–7.
- Zhou GK, Zhong R, Himmelsbach DS, McPhail BT, Ye ZH. Molecular characterization of PoGT8D and PoGT43B, two secondary wall-associated glycosyltransferases in poplar. *Plant Cell Physiol* 2007;48:689–99.